Journal of Alloys and Compounds 519 (2012) 136–139

Contents lists available at SciVerse ScienceDirect

Journal of Alloys and Compounds

journal homepage: www.elsevier.com/locate/jallcom

Fabrication of lanthanide decatungstate $[Ln^{III/IV}(W_5O_{18})_2]^{8-/9-}$ ($Ln = Ce^{IV/III}$, Eu^{III}, and Er^{III}) thin films using spin-coating from aqueous solutions

Yusuke Fujita [a], Noritaka Ishihara [a], Keisuke Fukaya [b], Atthapon Srifa [b], Haruo Naruke [a,*]

[a] Chemical Resources Laboratory, Tokyo Institute of Technology, 4259 Nagatsuta, Midori-ku, Yokohama 226-8503, Japan
[b] National Nanotechnology Center (NANOTEC), 111 Thailand Science Park, Paholyothin Rd, Klong 1, Klong Luang, Phathumthani 12120, Thailand

ARTICLE INFO

Article history:
Received 18 October 2011
Received in revised form
26 December 2011
Accepted 27 December 2011
Available online 3 January 2012

Keywords:
Polyoxometalate
Spin-coating
Lanthanide
Photoluminescence
X-ray diffraction
Self-organization

ABSTRACT

Lanthanide decatungstate $Na_m[Ln(W_5O_{18})_2]\cdot nH_2O$ (LnW_{10}: $m = 9$ for $Ln = Eu^{III}$, Ce^{III}, and Er^{III}; $m = 8$ for $Ln = Ce^{IV}$) thin films were fabricated on quartz glass substrates by spin-coating using water as the solvent. In this method, we exclude hybrids with organic materials to avoid undesirable modification of the original photophysical properties of LnW_{10}. The resultant films were characterized by X-ray diffraction (XRD), scanning probe microscopy (SPM), optical absorption, and photoluminescence spectroscopy. All the films had high transparency, flatness, and homogeneity. The thickness of the films was controllable by adjusting the concentration of LnW_{10} solution. XRD measurements showed that the $[Ln^{III/IV}(W_5O_{18})_2]^{9-/8-}$ molecules in all the films were self-organized, forming a layer-like periodic structure with a periodicity of ~14 Å in the early stage, followed by time-dependent structural changes. The $Eu^{III}W_{10}$ film exhibited photoluminescence upon excitation at ~250 nm; the film's spectrum and lifetime were similar to those of the crystal sample. These results demonstrate that the molecular environment in LnW_{10} thin films is similar to that found in solid crystals.

1. Introduction

Polyoxometalates (POMs) are inorganic polynuclear clusters consisting mainly of edge and corner-shared metal-oxygen polyhedrons [1,2]. The compositional and structural diversity of POMs enable a variety of physicochemical properties such as catalytic, physiological, optical, magnetic, and redox behavior [3]. One current interest lies in the immobilization and orientation control of POM molecules for application to functional nano-structured devices. Unlike general metal-oxide crystals, most POM crystals contain a large number of solvent molecules and are not suitable for direct use as functional materials. In recent years, several methods for the immobilization of POM thin films on solid substrates have been developed. The current trend followed by POM-film formation techniques is to utilize nano-structured hybrids consisting of POMs and organic materials, which are well exemplified by Langmuir–Blodgett (LB) and layer-by-layer (LbL) methods [4–6]. These methods have remarkable advantages in controlling the molecular arrangement and orientation in the films, where functions of POMs and organic materials can be combined. However, in some cases, the formation of a hybrid with organic substances may suppress certain features of POMs. For example, photoluminescent lanthanide-containing POMs such as $[Ln(W_5O_{18})_2]^{m-}$ and $[Ln(XM_{11}O_{39})_2]^{n-}$ ($Ln = Eu^{III}$, Tb^{III}; $X = B^{III}$, Si^{IV}, P^{V}; $M = W^{VI}$, Mo^{VI}) in LB and LbL films and in composites with organic cations exhibit lower luminescence intensities than expected. This is because of the low content of the POMs resulting from dilution with bulky organic molecules [7–9] and/or non-radiative deactivation pathways through organic functional groups [10]. Furthermore, in most cases, an interaction between POM molecules and organic cations in multilayers induces remarkable molecular distortions that result in changes in the emission spectra [7–10].

Herein, we describe the fabrication of pure, inorganic POM thin films on quartz glass substrates by means of a simple spin-coating method using aqueous solutions of POMs taking advantage of their water solubility. Because this method does not require the formation of a composite with organic substances, the POM anions are expected to be located in ambient environments similar to the environments in inorganic crystals. In this study, we fabricated thin films of sodium salts of Ln decatungstate $Na_m[Ln(W_5O_{18})_2]\cdot nH_2O$ (LnW_{10}: $m = 9$ for $Ln = Eu^{III}$, Ce^{III}, and Er^{III}; $m = 8$ for $Ln = Ce^{IV}$). $Eu^{III}W_{10}$ is known to exhibit strong photoluminescence of Eu^{3+} under ultraviolet excitation, and its spectrum is sensitive to a change in the ligand field of Eu^{3+} induced by molecular distortion [11–15]. Therefore, $Eu^{III}W_{10}$ is a favorable material to be used for evaluating the molecular environment in thin films. In order to evaluate the effects of molecular size and anion charge of POMs,

* Corresponding author. Tel.: +81 045 924 5271; fax: +81 045 924 5271.
E-mail address: hnaruke@res.titech.ac.jp (H. Naruke).

0925-8388/$ – see front matter © 2012 Elsevier B.V. All rights reserved.
doi:10.1016/j.jallcom.2011.12.140

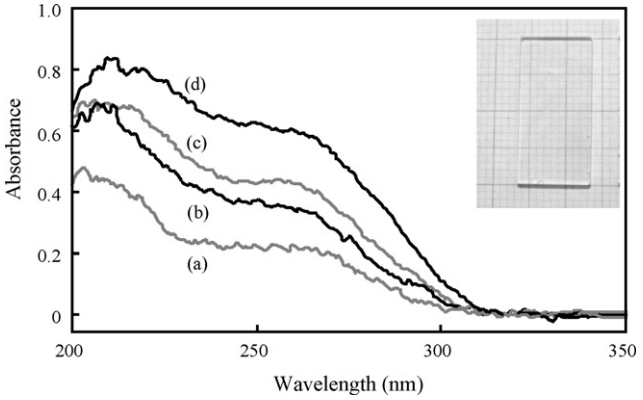

Fig. 1. UV spectra of $Eu^{III}W_{10}$ films fabricated with various concentrations of casting POM solutions. (a) 0.1 g/ml; (b) 0.2 g/ml; (c) 0.3 g/ml; and (d) 0.5 g/ml. Inset: image of transparent $Eu^{III}W_{10}$ film on quartz glass substrate.

the characteristics of three isotypic LnW_{10} films, where Ln = Eu^{III}, $Ce^{III/IV}$, and Er^{III}, are compared. To the best of our knowledge, this is the first example of direct fabrication of POM films in the form of inorganic salts.

2. Experimental

2.1. Sample preparation

The sodium salts of Ln decatungstate, $Na_m[Ln(W_5O_{18})_2]\cdot nH_2O$ (LnW_{10}: $m = 9$ for Ln = Eu^{III}, Ce^{III}, and Er^{III}; $m = 8$ for Ln = Ce^{IV}) were synthesized according to the method reported by Sugeta and Yamase [15]. Solutions of LnW_{10} were then prepared by dissolving the LnW_{10} crystals (0.05–0.25 g) in distilled water (0.5 ml).

2.2. Fabrication of films

Quartz glass substrates ($20 \times 10 \times 1$ mm) were ultrasonically cleaned with a detergent solution, rinsed three times with distilled water, and washed with acetone (for 10 min each). To increase their hydrophilicity, the substrates were then treated with a glow discharge using an ion sputtering device (JEOL JFC-1100E) with a discharge current of 10 mA for 5 min under reduced pressure. LnW_{10} thin films were made using a temperature-controllable spin-coater (Imoto machinery) according to the following procedure. The quartz glass substrate was set on a rotation stage that had been heated to 45 °C. Two or three drops of aqueous LnW_{10} solution (0.1–0.5 g/ml) were added to the top of the substrate, which was then cast at a spinning rate of 2500 rpm for 30 s.

2.3. Measurements

Powder X-ray diffraction (XRD) (Rigaku RINT-2100) was carried out on all films. The surface topography of the films was observed by using a scanning probe microscope (SEIKO Instruments, SPA300HV) operating in dynamic force mode and the thickness was measured by a profilometer (Veeco, DEKTAK3ST). UV–vis spectra were recorded on a spectrophotometer (JASCO V-570). Glow-discharge optical emission spectroscopy (GD-OES) (Jobin Yvon, JY-5000RF) was carried out for the $Ce^{IV}W_{10}$ film, which enabled the measurement of elemental distribution as a function of depth from the film surface. A photoluminescence spectrum for the $Eu^{III}W_{10}$ film was recorded at room temperature using a fluorescence spectrometer (HITACHI F-4500). Decay of the $^5D_0 \rightarrow {}^7F_1$ emission (593 nm) of Eu^{3+} was obtained using a system comprising a 266-nm pulse laser (Nd:YAG, Litron N250T-20FHG), a monochromator (Spex 270M) equipped with a photomultiplier (Hamamatsu R3896), and an oscilloscope (Iwatsu DS-8608).

3. Results and discussion

3.1. Optical, morphological, and compositional properties

All the fresh $Ln^{III/IV}W_{10}$ films are highly transparent with light transmittances (>400 nm) over 90%. The UV–vis absorption spectrum of the $Eu^{III}W_{10}$ film is shown in Fig. 1(a). The spectrum shows a broad O → W LMCT band of the $[W_5O_{18}]^{6-}$ unit at <300 nm; this result is in agreement with that of the spectrum of $Eu^{III}W_{10}$ in aqueous solution [14]. The morphology of the $Eu^{III}W_{10}$ film was observed by SPM (Fig. 2). Surface RMS (root mean square) of the film

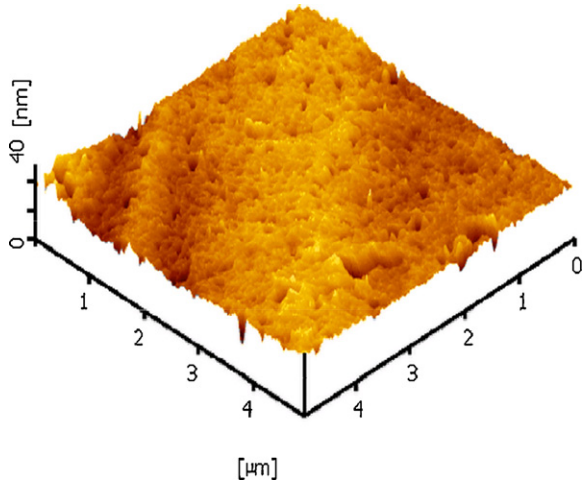

Fig. 2. SPM image of $Eu^{III}W_{10}$ film surface.

with a thickness of ~60 nm was 3.5 nm, demonstrating that the film surface has only a slight roughness. The result of the GD-OES measurement for the $Ce^{IV}W_{10}$ film is shown in Fig. 3. Although a small condensation of Na is seen near the film surface and film/substrate interface, W and Ce distribute homogeneously throughout the cross section of the material. These results demonstrate that the spin-coating process can produce POM films with high transparency, smoothness, and homogeneity. It should be noted that the films lost part of their transparency when they were stored under atmospheric conditions (refer to the following section).

3.2. XRD patterns

Fig. 4(a), (d), and (g) show XRD patterns of the as-prepared LnW_{10} films (Ln = Eu^{III}, Ce^{III}, Ce^{IV}). The diffraction pattern of the $Eu^{III}W_{10}$ film (Fig. 4(a)) consists of peaks at $2\theta = 6.28°$, 12.68°, 19.06°, 25.68°, and 32.3°, which correspond to 00l (l = 1–5) reflections with a periodicity of $d = 13.9$ Å. It should be noted that the pattern does not agree with a simulated pattern of a $Eu^{III}W_{10}$ crystal [15] and reveals a self-organization of the $[Eu^{III}(W_5O_{18})_2]^{9-}$ anions to form a unique layer-like periodic structure. Other thin films, namely $Ce^{III}W_{10}$, $Ce^{IV}W_{10}$, and $Er^{III}W_{10}$, showed similar XRD patterns (Figs. 4(d), (g) and S1) with d-spacings of 14.3, 14.4, and 13.7 Å, respectively. It is of significance that the POM films formed without

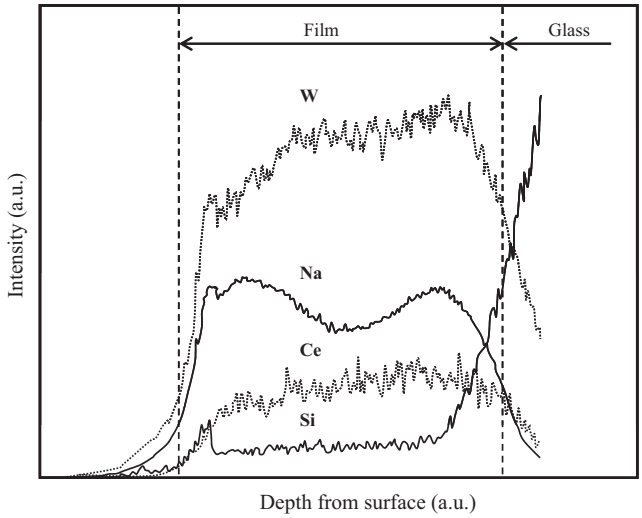

Fig. 3. Element distributions in $Ce^{IV}W_{10}$ film measured by GD-OES.

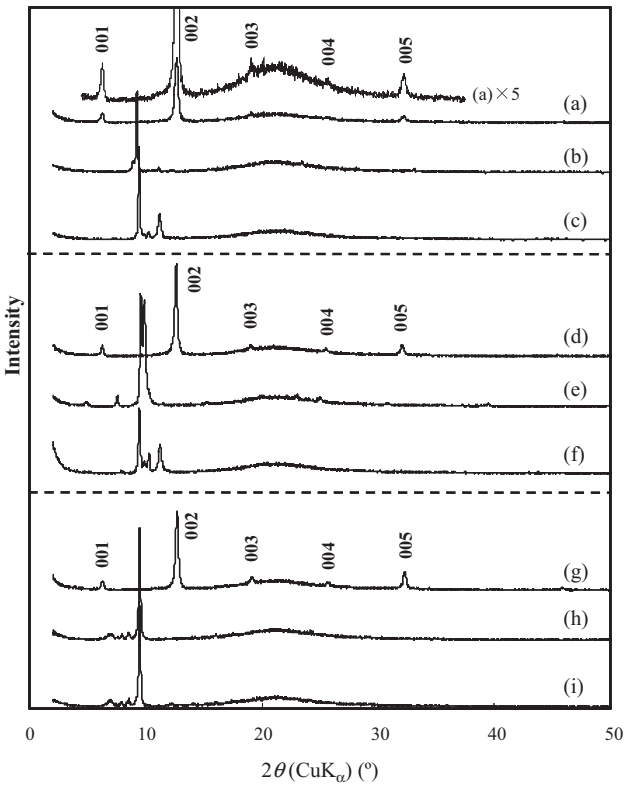

Fig. 4. Time-evolutions of XRD patterns of LnW_{10} films $Eu^{III}W_{10}$: (a) 0 h; (b) 48 h; and (c) 168 h. $Ce^{III}W_{10}$: (d) 0 h; (e) 24 h; and (f) 168 h. $Ce^{IV}W_{10}$: (g) 0 h; (h) 45 h; and (i) 168 h.

an organic–inorganic hybrid exhibited such self-organized periodic structures. The LB and LbL films composed of multilayers of organic molecules and $[Eu^{III}(W_5O_{18})_2]^{9-}$ anions have been shown to have much longer periodicities (21–49 Å) [7,18]. It is strongly suggested that the $[Ln^{III/IV}(W_5O_{18})_2]^{9-/8-}$ anions be arranged in layers with a *d*-spacing of ~14 Å, and that the Na^+ ions occupy the interstitials of the anions for charge compensation. Taking the anion size (~15 × 8 Å) into account, the *d*-spacing can accommodate single or double layers of the anions. Because all the LnW_{10} films show similar initial XRD patterns and *d* values, it is clear that the anionic charge and ionic radius of $Ln^{III/IV}$ only have a small influence on the self-organization and periodicity.

It was found that the initial XRD patterns of these films changed dynamically with time when the films were stored in an atmospheric environment. The initial pattern of the $Eu^{III}W_{10}$ film disappeared and was replaced by several new peaks (Fig. 4(b)). Finally, approximately seven days after film preparation, the diffractogram showed a dominant peak at $2\theta = 9.44^\circ$ and other smaller peaks at higher angles (Fig. 4(c)). Similar behavior was observed for the $Ce^{III}W_{10}$ film (Fig. 4(d)–(f)). We have not succeeded in indexing these transient and final XRD peaks. Such remarkable variation in the diffractograms indicates a rearrangement of the $[Ln^{III}(W_5O_{18})_2]^{9-}$ anion. On the other hand, the diffractogram of the $Ce^{IV}W_{10}$ film changed in a different manner, as shown in Fig. 4(g)–(i). Here, the final pattern consists of an intense diffraction at $2\theta = 9.48^\circ$ with other weaker peaks at lower angles. The difference in the charge of the $[Ln^{III/IV}(W_5O_{18})_2]^{9-/8-}$ anion is suggested to influence the rearrangement process owing to different electrostatic interactions between the anions and the Na^+ cations. It is worth noting that these variations in the diffractograms occurred with turbidity in the films; the turbidity led to a slight decrease in transparency. Prolonged storage (several weeks) in humid air gave rise to further loss of transparency, retaining

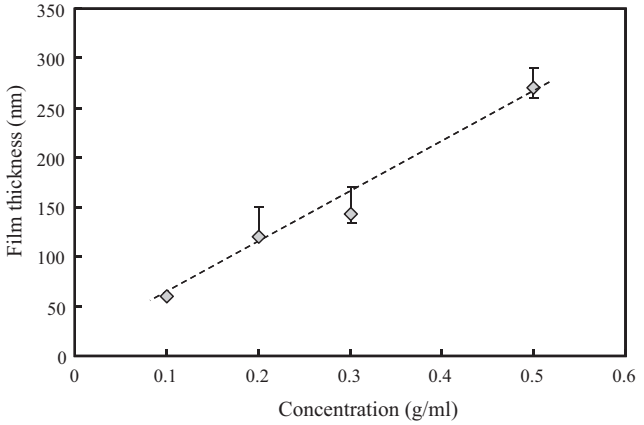

Fig. 5. The relationship between thickness of $Eu^{III}W_{10}$ films and concentration of casting solutions.

the final XRD patterns shown in Fig. 4(c), (f), and (i). When the as-prepared films were stored in a vacuum desiccator, no such behavior was observed and the initial patterns (Fig. 4(a), (d), and (g)) remained unchanged for at least four months. We ascribe that water molecules absorbed by the films induced the rearrangement of the anions.

3.3. Film thickness

The control of film thickness was studied for the $Eu^{III}W_{10}$ film by changing the concentration of the POM solutions in the range 0.1–0.5 g/ml. The 0.1 g/ml solution resulted in a film thickness of approximately 60 nm. When the concentration was increased to 0.5 g/ml, under the same spin-coating conditions, the thickness increased proportionally to ~270 nm (Fig. 5). The increase in the film thickness was reflected by a gradual growth of the O → W LMCT band in the absorption (Fig. 1) and photoluminescence excitation (Section 3.4) spectra. Thus, the film thickness is controllable to some extent simply by adjusting the POM concentration of the casting solution. Furthermore, the thickness had no effect on the initial XRD patterns (Fig. S2).

3.4. Photoluminescence properties of the $Eu^{III}W_{10}$ film

The crystalline solid of $Eu^{III}W_{10}$ film shows bright photoluminescence owing to f–f transitions in Eu^{3+} under photoexcitation into O → W LMCT and f–f bands [11–15]. In this work, we recorded emission and excitation spectra of the $Eu^{III}W_{10}$ thin film and compared them to those of the crystalline solid. It is remarkable that photoluminescence spectra of the film and crystals are quite similar (Fig. 6). The spectral peaks are assigned to $^5D_0 \rightarrow {}^7F_1$ (588, 593 nm), $^5D_0 \rightarrow {}^7F_2$ (613, 617 nm), $^5D_0 \rightarrow {}^7F_3$ (648 nm), $^5D_0 \rightarrow {}^7F_4$ (688, 697 nm) within the $4f^6$ configuration of Eu^{3+}. It is well known that the relative intensity of the $^5D_0 \rightarrow {}^7F_2$ transition to that of $^5D_0 \rightarrow {}^7F_1$ strongly reflects the ligand-field of Eu; this transition is referred to as a "hypersensitive" transition [13]. The $^5D_0 \rightarrow {}^7F_2$ transition is forbidden in an ideal D_{4d} point symmetry of a free $[Eu^{III}(W_5O_{18})_2]^{9-}$ anion. In the sodium salt, the anion is slightly distorted and the $^5D_0 \rightarrow {}^7F_2$ transition is partially allowed because of vibronic effect at room temperature and a small deviation in C_{4v} symmetry [13,15], resulting in weak intensity (Fig. 6(a)). The $^5D_0 \rightarrow {}^7F_1$ luminescence of the film showed an exponential decay (Fig. 6 inset) with a lifetime of 3.0 ms, which is consistent with that of the $Eu^{III}W_{10}$ solid at room temperature (2.9 ms) [14]. It should be noted that many hybrid films consisting of $[Eu^{III}(W_5O_{18})_2]^{9-}$ and organic molecules prepared by means of LB and LbL methods showed significantly larger relative intensity of the $^5D_0 \rightarrow {}^7F_2$

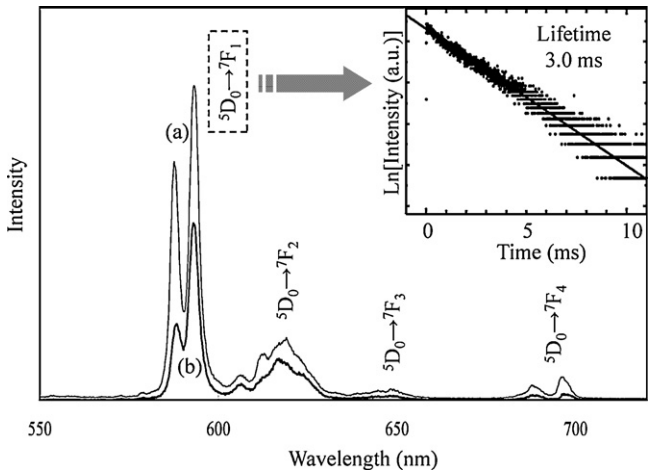

Fig. 6. Photoluminescence spectra of $Eu^{III}W_{10}$ crystals (a) and film (b) at room temperature under 260-nm excitation. Inset: decay of $^5D_0 \rightarrow {}^7F_1$ luminescence under 266-nm excitation.

emission and shorter lifetimes than the $Eu^{III}W_{10}$ solid [7,16–18]. These facts suggest that a sizable distortion of the $[Eu^{III}(W_5O_{18})_2]^{9-}$ anion (viz., reduction of the ligand-field symmetry around Eu) occurs in the hybrid films, probably due to the highly anisotropic electrostatic potential in inorganic/organic multilayers. The shorter lifetime has been presumed to be due to enhanced $^5D_0 \rightarrow {}^7F_2$ transition probability by symmetry reduction of the Eu center. The reduction of emission lifetimes in POM/organic hybrid films was observed not only for the $[Eu^{III}(W_5O_{18})_2]^{9-}$ anion but also for other Eu-containing POMs [19].

The excitation spectrum of the $Eu^{III}W_{10}$ crystal (Fig. 7(a)) consists of a broad O → W LMCT excitation band around 330 nm and sharp peaks in the >350 nm region due to direct f–f excitation of Eu. The former band demonstrates an efficient intermolecular energy transfer from the $[W_5O_{18}]^{6-}$ unit to the Eu center, even at room temperature [13,14]. In the film (Fig. 7(b)), the O → W LMCT excitation band is centered at around 275 nm, while the direct f–f excitation bands are unobservable. As the film thickness is gradually increased to ~270 nm, the O → W LMCT band is enhanced proportionally to the thickness (Fig. S3). However, the f–f bands remain too weak to be observed. The weak, direct f–f excitation bands can be explained in terms of their low absorption coefficients due to forbidden transitions. In a highly transparent thin film, few Eu centers can be excited, whereas in the powder sample, which has a larger thickness, the excitation light is diffused by multi-reflections to excite larger numbers of Eu atoms. The relatively low f–f bands and the blue-shift of the O → W LMCT band (Fig. 7(b)) have also been observed in LB and LbL films [7,16–18] and in aqueous solutions [14,20]. In summary, the $Eu^{III}W_{10}$ film fabricated by spin-coating retains the molecular environment present in the crystal.

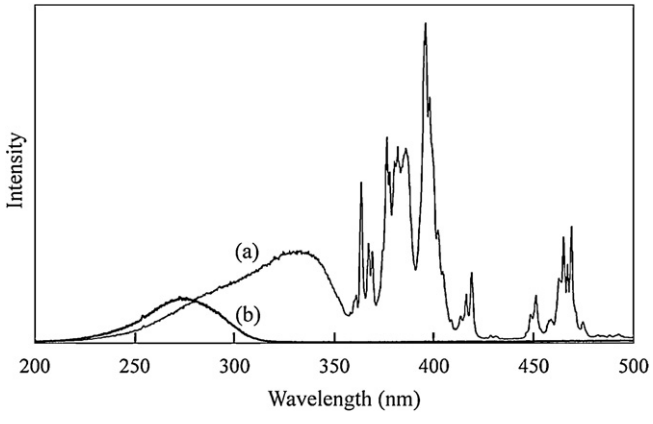

Fig. 7. Excitation spectra of $Eu^{III}W_{10}$ crystals (a) and film (b) for monitoring $^5D_0 \rightarrow {}^7F_1$ luminescence (593 nm).

4. Conclusions

We obtained flat, homogeneous, and transparent thin films of LnW_{10} by using temperature-controlled spin-coating from only aqueous solutions. The XRD measurements showed that anions in the film were self-organized, forming a layer-like periodic structure on the quartz substrates. The film thickness is controllable in the range 60–270 nm by adjusting the concentration of the casting solution. The photoluminescence spectrum and lifetime of the $Eu^{III}W_{10}$ film were comparable to those in the crystalline sample, demonstrating that the molecular environment in the crystal is retained in the film. This result is in contrast with that of the inorganic/organic hybrid-type LB and LbL films containing $[Eu^{III}(W_5O_{18})_2]^{9-}$, which are distorted, resulting in different luminescence properties from those of the crystalline sample. We are currently analyzing the initial self-organized structure of the $[Ln^{III/IV}(W_5O_{18})_2]^{9-/8-}$ anions. In future work, it will be of interest to study temperature effects (which include preheating of substrates and film annealing after coating) on various film properties. Our process is considerably simple and applicable to other substrate materials. Preliminary attempts to form films on ITO and flexible organic polymer substrates have been successful. For practical application to functional devices, there remain some challenges to be overcome, e.g., prevention of film deterioration, control of molecular orientation, and deposition of multilayers of POMs and other inorganic materials.

Acknowledgments

This work is partially supported by the research foundation from KRI, Inc. The authors wish to thank Dr. T. Fukui and Dr. H. Kawasaki at KRI for their helpful discussion. Thanks are also due to Dr. A. Genseki at the Center for Advanced Materials Analysis in our institute for the measurement of GD-OES.

Appendix A. Supplementary data

Supplementary data associated with this article can be found, in the online version, at doi:10.1016/j.jallcom.2011.12.140.

References

[1] M.T. Pope, Heteropoly and Isopoly Oxometalates, Springer, Berlin, 1983.
[2] M.T. Pope, A. Müller, Angew. Chem. Int. Ed. Engl. 30 (1991) 34.
[3] C.L. Hill (Ed.), Chem. Rev. 98 (1998) 1.
[4] M. Clemente-León, E. Coronado, A. Soriano-Portillo, C. Mingotaud, J.M. Dominguez-Vera, Adv. Colloid Interface Sci. 116 (2005) 193.
[5] S. Liu, D. Volkmer, D.G. Kurth, J. Cluster Sci. 14 (2003) 405.
[6] S. Liu, Z. Tang, Nano Today 5 (2010) 267.
[7] Y. Wang, X. Wang, C. Hu, C. Shi, J. Mater. Chem. 12 (2002) 703.
[8] L. Xu, H. Zhang, E. Wang, A. Wu, Z. Li, Mater. Lett. 54 (2002) 452.
[9] L. Xu, H. Zhang, E. Wang, A. Wu, Z. Li, Mater. Chem. Phys. 77 (2003) 484.
[10] T.R. Zhang, C. Spitz, M. Antonietti, C.F.J. Faul, Chem. Eur. J. 11 (2005) 1001.
[11] R.D. Peacock, T.J.R. Weakley, J. Chem. Soc. A (1971) 1937.
[12] M.J. Stillman, A.J. Thomson, J. Chem. Soc., Dalton Trans. (1976) 1138.
[13] G. Blasse, G.J. Dirksen, F. Zonnevijlle, J. Inorg. Nucl. Chem. 43 (1981) 2847.
[14] R. Ballardini, Q.G. Mulazzani, M. Venturi, F. Balletta, V. Balzani, Inorg. Chem. 23 (1984) 300.
[15] M. Sugeta, T. Yamase, Bull Chem. Soc. Jpn. 66 (1993) 444.
[16] M. Jiang, X. Zhai, M. Liu, Langmuir 21 (2005) 11128.
[17] J. Wang, H. Wang, L. Fu, F. Liu, H. Zhang, Thin Solid Films 415 (2002) 242.
[18] T. Ito, H. Yashiro, T. Yamase, J. Cluster Sci. 17 (2006) 375.
[19] J. Wang, H. Wang, F. Liu, L. Fu, H. Zhang, J. Lumin. 101 (2003) 63.
[20] R.A. Sá Ferreira, S.S. Nobre, C.M. Granadeiro, H.I.S. Nogueira, L.D. Carlos, O.L. Malta, J. Lumin. 121 (2006) 561.